

Oscillatory Instabilities during the Electrocatalytic Oxidation of Methanol on Platinum

Andre L. Martins, Bruno C. Batista, Elton Sitta and Hamilton Varela*

Instituto de Química de São Carlos, Universidade de São Paulo, CP 780, CEP 13560-970 São Carlos-SP, Brazil

Descreve-se neste artigo a observação experimental de dinâmica oscilatória durante a oxidação eletrocatalítica de metanol sobre platina. Além das, previamente relatadas, oscilações de potencial, oscilações de corrente obtidas sob controle potencioestático também são apresentadas. A região de existência de oscilações de corrente é mapeada no plano de bifurcação voltagem aplicada x resistência. Conjuntamente com investigações eletroquímicas, espectroscopia FTIR *in situ* também foi aplicada nestes estudos. Apesar de não ter sido possível acompanhar eventuais variações de intermediários reacionais durante as oscilações, tais experimentos revelaram que a cobertura média de monóxido de carbono permanece consideravelmente alta durante as oscilações. Os resultados são discutidos e comparados com as oscilações observadas na eletrooxidação de ácido fórmico, um sistema cujo comportamento é mais entendido e amplamente fundamentado por dados espectroscópicos obtidos *in situ*.

It is described in this paper the experimental observation of oscillatory dynamics during the electrocatalytic oxidation of methanol on platinum. Besides the previously reported potential oscillations, current oscillations obtained under potentiostatic control are also presented. The existence region of current oscillations is mapped in an applied voltage x resistance bifurcation diagram. Conjointly with electrochemical investigations, *in situ* FTIR spectroscopy was also employed in the present studies. Although we were not able to follow eventual intermediate coverage changes during the oscillations, those experiments revealed that the mean coverage of adsorbed carbon monoxide remains appreciably high along the oscillations. Results are discussed and compared with the oscillations observed in the electrooxidation of formic acid, a system whose behavior is more understood and widely supported by *in situ* spectroscopic data.

Keywords: current and potential oscillations, methanol, electrocatalysis, *in situ* FTIR

Introduction

Methanol has been pointed as one of the most promising organic molecules to be used in large scale energy conversion systems, as in the so-called direct methanol fuel cells (DMFC).¹⁻³ Limitations associated to the high overpotential and the existence of parallel reaction pathways makes its understanding a rather challenging task. Studies have been carried out mainly on platinum surfaces, both polycrystalline and single crystals, by means of different electrochemical approaches sometimes coupled to other *in situ* and *on line* techniques.⁴⁻¹⁶ In most of these reports, the focus stands on the electrocatalytic aspects of the methanol oxidation and encompasses questions such as the relationship between reaction rate and applied potential, the impact of the interfacial structure on reaction rate and

selectivity, and the nature and geometry of adsorbates, to list a few. By far less studied however are the issues related to the complex kinetic aspects associated to the electrooxidation of methanol.

In one of the first reports on the instabilities in the electrooxidation of methanol on platinum and in sulfuric acid media, Buck and Griffith¹⁷ observed potential oscillations under galvanostatic control. Krausa and Vielstich¹⁸ demonstrated the influence of methanol residues at the platinum electrode surface on the galvanostatic potential oscillations. Those experiments were carried out using 0.5 mol L⁻¹ of methanol dissolved in aqueous 0.5 mol L⁻¹ of HClO₄ media. Transitions to temporal chaos by period doubling in the electrooxidation of 1 mol L⁻¹ of CH₃OH on platinum in 0.5 H₂SO₄ electrolyte at 43 °C and under galvanostatic control were reported by Okamoto and co-workers.¹⁹ Using electrochemical impedance spectroscopy, Lee *et al.*^{20,21} discussed the

*e-mail: varela@iqsc.usp.br

presence of temporal instabilities in the platinum/sulfuric acid/methanol system and identified a region of hidden negative differential resistance as primarily responsible for the occurrence of oscillations. In a series of papers, Schell and co-workers investigated the presence of other instabilities during the electrooxidation of methanol on platinum, including the experimental observation of complex cyclic voltammograms in low conductivity media²² and multi-stability.^{23,24} It should be emphasized that, as far as the electrooxidation of methanol on *platinum* is concerned, only potential oscillations have been reported so far (for a review, see references^{25,26}). Very few works report the occurrence of current oscillations in this reaction. Hachkar *et al.*²⁵ observed potentiostatic oscillations in the electrooxidation of methanol on rough rhodium surfaces (roughness of about 100). The experiments were performed in alkaline media and at temperature above 55 °C. Vielstich and co-workers²⁷ observed current oscillations in the course of the potentiostatic oxidation of methanol on platinum based gas diffusion electrodes. Instabilities in this case were observed at high applied voltages (> 1.0 V *vs.* RHE) and were attributed to the non-electrochemical step of diffusion inside the electrode pores.²⁷

When compared to other C1 molecules such as formaldehyde and formic acid, the electrooxidation of methanol can be considered as less susceptible to oscillatory instabilities. Indeed, the potential oscillations reported for methanol electrooxidation are usually in the range of 200-300 mV of amplitude and with periods of about 1 to 15 s.^{18,19,21} Moreover, the oscillatory patterns are considerably simple. Those features are rather astonishing if one considers the plethora of oscillatory patterns observed for instance in the electrooxidation of formic acid.²⁸⁻³⁴

In the present work we report the investigation of the oscillatory instabilities in the methanol electrooxidation reaction on a polycrystalline platinum electrode and in aqueous sulfuric acid media. Besides conventional electrochemical experiments under potentiostatic and galvanostatic control, *in situ* FTIR spectroscopy was also employed to quantify the mean carbon monoxide coverage during the oscillations. The results are discussed in connection with those observed for the, more extensively studied, formic acid system.

Experimental

General

Sulfuric acid (Mallinckrodt, 99.8%), and methanol (J.T. Baker, 99.9%) were used without further purification and all solutions were prepared with high purity water

(18.2 MΩ.mm, Milli-Q system, Millipore). The reference electrode was a reversible hydrogen electrode, and all potentials are quoted with respect to it (RHE). In all experiments the cell atmosphere was kept free of oxygen by argon (White Martins 99.99 %) or nitrogen (White Martins 99.996 %) bubbling. All experiments were carried out at room temperature, 25 °C. Prior to each experiment, the working electrode (WE) was cycled between 0.05 and 1400 mV at 100 mVs⁻¹ for about one hour in order to assure a reproducible behavior.^{35,36}

Conventional experiments

In all conventional electrochemical experiments, a polycrystalline platinum disk (6.5 mm in diameter and geometric area of 0.32 cm²) embedded in a Teflon body was used as working electrode (WE). A large area platinum flag bent in a ring shape and symmetrically placed below the WE served as a counter electrode (CE). The electrochemical experiments were performed with a FAC 2001 potentiostat/galvanostat coupled to a Princeton Applied Research sweep generator Model 175.

In situ FTIR experiments

FTIR experiments were performed with a Nicolet spectrometer, model Nexus 670, equipped with a MCT detector. The spectro-electrochemical cell was fitted with a 60° CaF₂ prismatic window, as described elsewhere.³⁷ A Solartron potentiostat model SI 1287 was used in these experiments. The experiments were performed using the thin layer configuration, where the platinum surface, *i.e.* the WE, is pressed against the prismatic window.

Results and Discussion

Figure 1 shows the potential oscillations observed during the electrooxidation of methanol (0.68 mol L⁻¹) on platinum in sulfuric acid media (0.49 mol L⁻¹), under galvanostatic control. Low-amplitude harmonic oscillations sets in at about 200 μA via a supercritical Hopf-bifurcation.³⁸ Initial increase of the applied current implies increasing the oscillation amplitude as given in Figure 1(a), (b) and (c). For applied currents between 285 and 300 μA, a second bifurcation leading to a period doubled structure takes place. The time series illustrated in Figure 1(d) exemplifies this behavior and is characterized by a small modulation in the passive (high U values) branch of the oscillation. Further increase of the applied current leads to an additional modulation in the upper part of the oscillation cycle indicating a period three or

even a I^2 pattern, where the notation accounts for 1 large amplitude oscillation intercalated with 2 small amplitude ones. Finally, the time series depicted in Figure 1 shows a flatter high potential state. With additional increase in the applied current the system undergoes a saddle-loop bifurcation where the limit-cycle collides with a fixed point relative to the oxygen evolution reaction branch, similarly to that observed during the electrooxidation of hydrogen under similar conditions.^{39,40}

Overall, the electrode potential varies from about 650 to 850 mV. Accompanying the decreasing in the harmonic character of the potential oscillation the system is found to spend more time in the passive state at higher applied current. The oscillation period increases from *ca.* 2 to 4 s for increasing current. Potential oscillations during the electrooxidation of methanol on platinum have been previously observed.¹⁷⁻²¹ Besides conventional oscillations similar to the ones given in Figure 1, Krausa and Vielstich¹⁸ also observed larger amplitude oscillations ($540 < U < 870$ mV) with periods in the range of about

5 min. Those patterns are considerably unusual and were observed only after a second induction period of 20 min following the end of the first, regular, oscillations. Such oscillations were observed when a pre-treatment at -30 μA prior to the current step to 1.8 mA was performed. The fact that such high potential oscillations have not been observed in our system could be discussed in terms of the use of sulfuric acid in our experiments instead of perchloric acid as in their case.¹⁸ As fully reported,^{14,16,41} the adsorption of (bi)sulfate anion can considerably inhibit methanol adsorption and thus its oxidation, resulting in smaller current under potentiostatic control. Under galvanostatic control the presence of strongly adsorbing anions would result in an inhibition of the reaction branch which in turn would favor the collision with the fixed point in the oxygen evolution branch.

Lee *et al.*^{20,21} observed similar potential oscillation in the electrooxidation of CH_3OH (0.03 mol L^{-1}) in HClO_4 (0.1 mol L^{-1}) on platinum surface. The authors used electrochemical impedance spectroscopy and identified a

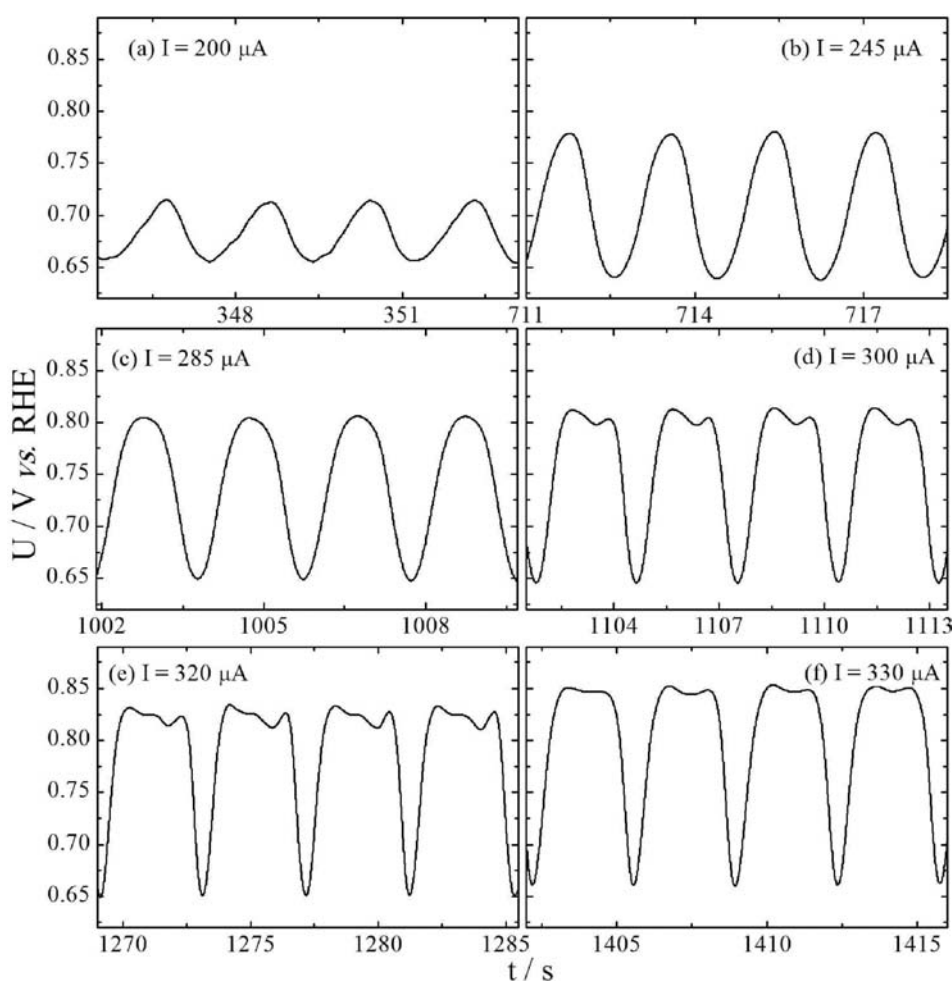


Figure 1. Potential time series under galvanostatic control. Electrolyte: $[\text{CH}_3\text{OH}] = 0.68$ mol L^{-1} and $[\text{H}_2\text{SO}_4] = 0.49$ mol L^{-1} .

negative differential resistance (NDR) region around the voltammetric peak of the positive going sweep. Once this NDR is not apparent in a stationary current/potential curve, it has been often named hidden NDR or HN-NDR.⁴²⁻⁴⁵ In this type of electrochemical oscillator the hidden NDR is associated to an N shaped current/potential curve, the electrode potential plays the role of activator and is involved in a positive feedback loop. Important to the present context is that such system is capable to oscillate also under potentiostatic conditions provided that a certain ohmic drop exists in the potentiostatic control circuit.⁴² This ohmic drop can be induced either by decreasing the electrolyte conductivity or by inserting an external resistance between the working electrode and the potentiostat. Changing the solution conductivity would bring some difficulties, namely: (i) changes in the chemistry of the system; (ii) limited range of resistances achievable; and (iii) the experimental inconvenience of changing the electrolyte solution for each experiment. In the present work, we decided to vary the external resistance and keep the electrolyte composition unchanged.

Figure 2 shows current oscillations observed during methanol electrooxidation for a total resistance (*i.e.*, the negligible, solution resistance plus the external resistance) $R_t = 1.75 \text{ k}\Omega$ and different applied voltages. Similarly to that given in Figure 1, oscillations are born via a supercritical Hopf bifurcation and grow in amplitude for increasing applied voltage up to about $90 \mu\text{A}$. As shown in plates (d)-(f), small amplitude modulations in the passive state (high potential in Figure 1 and low current in Figure 2) are also present under potentiostatic control. Aperiodic modulations (I^n states), Figure 2f, are rather unstable and appear only near the upper voltage limit of the oscillatory region.

The existence region of current oscillations during methanol electrooxidation can be traced in terms of a bifurcation or phase diagram in the U vs. R_t plane. Figure 3 shows such a diagram obtained under slow voltammetric sweep (1 mV s^{-1}) using the same procedure as previously described.⁴⁰ As already mentioned, a feature of this class of electrochemical oscillator is to oscillate under both potential and current control, the diagram depicted in

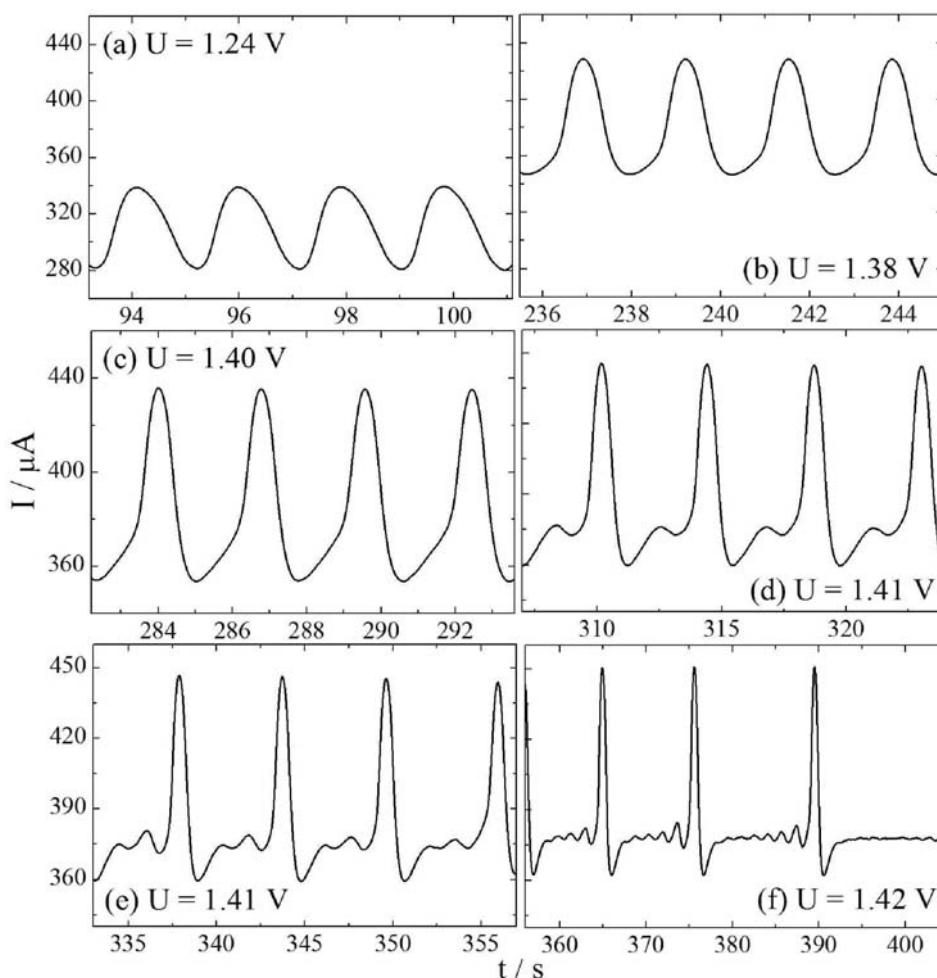


Figure 2. Current time series under potentiostatic control with $R_t = 1.75 \text{ k}\Omega$. Electrolyte: $[\text{H}_3\text{COH}] = 0.99 \text{ mol L}^{-1}$ and $[\text{H}_2\text{SO}_4] = 0.48 \text{ mol L}^{-1}$.

Figure 3 was obtained under potentiostatic control and the existence region of oscillations under galvanostatic operation would correspond to a situation where both voltage and resistance would be infinite.

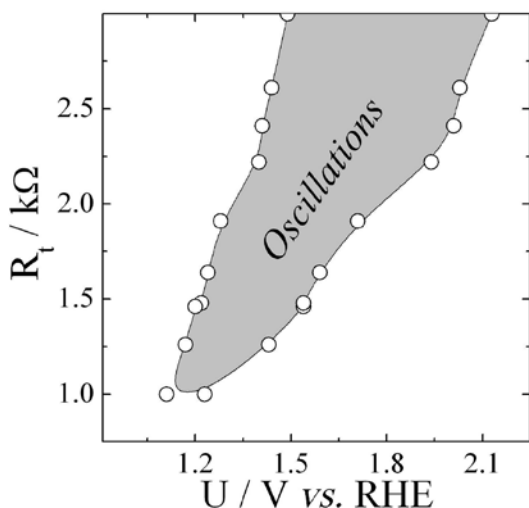


Figure 3. Bifurcation diagram in the R_t vs. U plane. Electrolyte: $[\text{H}_3\text{COH}] = 0.68 \text{ mol L}^{-1}$ and $[\text{H}_2\text{SO}_4] = 0.49 \text{ mol L}^{-1}$.

As already pointed out, the most intriguing aspects when comparing the oscillatory instabilities during the electrooxidation of methanol with those in other C1 molecules are the smaller oscillation amplitude and the simpler dynamic behavior of the former. Chen and Schell²⁴ argued that the reason for the electrooxidation of methanol be less susceptible to temporal instabilities is associated with the fact that the direct oxidation pathway *via* active intermediate is nearly negligible for this reaction. This explanation however is not supported by recent results reported by Iwasita and co-workers.¹⁴ In order to shed some light on the mechanistic features underlying this behavior, we have performed some *in situ* FTIR experiments during the electrooxidation of methanol under similar conditions of that presented in Figure 1. A set of IR spectra obtained as a function of time is presented in Figure 4a. The reference spectrum was taken at $U = 1400 \text{ mV}$. A small downwards band at around $2050\text{--}2070 \text{ cm}^{-1}$ relative to adsorbed carbon monoxide is discernible in every spectrum. Other existing features are the bands at 2280 and 2350 cm^{-1} which correspond to the asymmetric stretching mode of $^{13}\text{CO}_2$ and $^{12}\text{CO}_2$, respectively. These species were continuously formed along the galvanostatic experiment with a defined reaction rate. In those experiments, the electrode was subject to a pre-treatment at 1400 mV for 10 s and then to $U = 50 \text{ mV}$ for 30 s . The last seconds of polarization at 50 mV are given in Figure 4b for $t < 0 \text{ s}$, from $t = 0 \text{ s}$ on, the system was kept under galvanostatic control with application of a constant current of 4.5 mA . This applied current can be compared to

the situation given above in Figure 1 by taking into account the current density values as normalized by the geometric area, *i.e.* 1.1 mA cm^{-2} in Figure 4 and 0.74 mA cm^{-2} in Figure 1b.

The carbon monoxide coverage, θ_{CO} , defined as the ratio between the number of occupied and free surface atoms and given in terms of a fraction of a monolayer (ML), can be estimated as the ratio between the integrated bands around $2050\text{--}2070 \text{ cm}^{-1}$ at different times and that obtained for a full monolayer of CO_{ad} , calculated in a reference experiment. For the reference experiment, first the working electrode was polarized at 50 mV and the full CO_{ad} monolayer was built up during CO bubbling for 10 min ; afterwards the solution was purged with nitrogen for 30 min in order to remove the dissolved CO ; finally, the adsorbed CO was oxidized in a potential step to 900 mV . The surface saturation by carbon monoxide was confirmed by the suppression of hydrogen adsorption and it was assumed

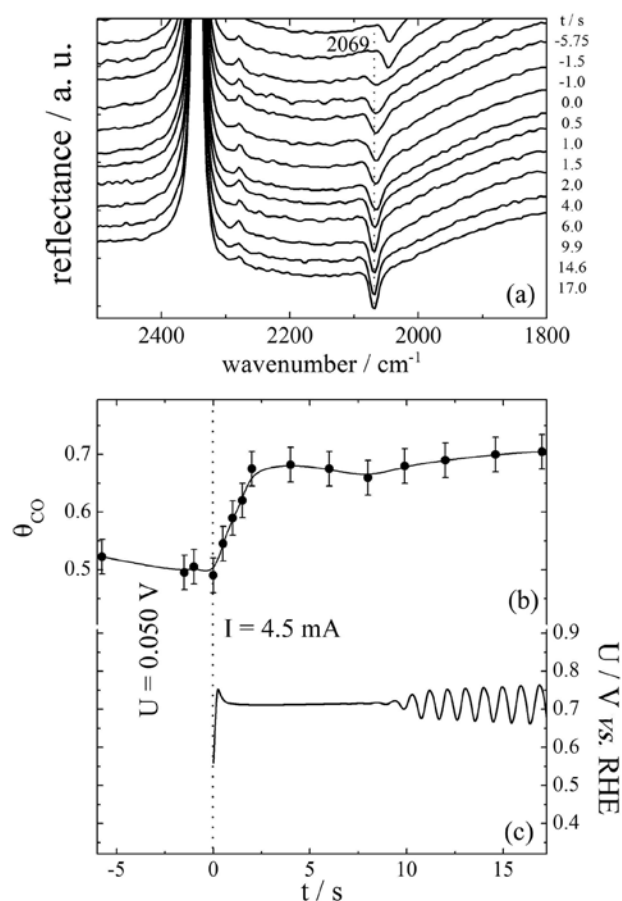


Figure 4. (a) FTIR spectra collected as a function of time in the course of methanol electrooxidation; (b) carbon monoxide coverage obtained from the integration of the band at 2069 cm^{-1} ; and (c) time evolution of the electrode potential. At $t < 0 \text{ s}$ the system was kept at $U = 50 \text{ mV}$, and from $t = 0 \text{ s}$ on, a constant current of 4.5 mA (or equivalently 1.1 mA cm^{-2} , see experimental section) was applied. Electrolyte: $[\text{H}_3\text{COH}] = 0.50 \text{ mol L}^{-1}$ and $[\text{H}_2\text{SO}_4] = 0.50 \text{ mol L}^{-1}$. The reference spectra was taken at $U = 1400 \text{ mV vs. RHE}$.

the linear relationship between coverage and band intensity. The faradaic charge associated to the electrooxidation of the carbon monoxide layer formed in the reference experiment corresponds to a coverage of 0.85 ML which means that the CO population under those conditions is composed by about 0.70 ML and 0.15 ML of linear (CO_L) and bridge (CO_B) coordinated adsorbed CO, respectively. This distribution can be easily obtained by the two equations: $\theta_{\text{CO-L}} + \theta_{\text{CO-B}} = 0.85 \text{ ML}$ and $\theta_{\text{CO-L}} + 2\theta_{\text{CO-B}} = 1 \text{ ML}$, and is in agreement to that reported by Osawa and co-workers⁴⁸ under similar conditions.

Figure 4b shows the carbon monoxide coverage as a function of time. At $U = 50 \text{ mV}$, θ_{CO} remains around 0.5 ML. After applying a constant current of 4.5 mA, a sharp increase up to about 0.68 ML is observed during the first 2.5 s. The CO coverage remains nearly constant all over the induction period and increases slightly when oscillations starts, at about 8 s. The time evolution of the electrode potential, U , is depicted in Figure 4c, and, as seen in Figure 1, the oscillations are rather harmonic and set in via a supercritical Hopf bifurcation. In spite of the differences in the working electrode and cell geometries, and in the thin layer configuration, oscillation amplitude and frequency are quite comparable to that given in Figure 1b. A slight periodic shift in the frequency of adsorbed carbon monoxide was also discernible in our experiments. The oscillations in the position of the CO_{ad} band were in-phase with that of the global time series, indicating that there is a periodic compression/relaxation in the CO_{ad} layer accompanying the potential oscillations. However, although the trend was clear, those oscillations were quite close to the resolution of our data, so that, no further analysis is possible. Along with the, already mentioned, continuous formation of CO_2 inside the thin layer, the oscillations in the position of the CO_{ad} band unambiguously prove that electrochemical oscillations are taking place also at the electrode surface at the thin layer. As previously reported by Honda *et al.*,⁴⁶ this is an important experimental concern when using the thin layer configuration.

Two important points can be extracted from Figure 4: (i) the increase observed in the carbon monoxide coverage during the induction period; and (ii) the value of $\theta_{\text{CO}} = 0.7 \text{ ML}$ around which oscillations are observed. Therefore, as clearly given in Figure 4(b)-(c) the increase in the carbon monoxide coverage can be ascribed as the main transformation experienced by the surface population during the induction period. The mean value of about 70% of a monolayer is very high and points to the fact that only a rather small portion of the electrode surface has its population changing during the oscillation. This could in principle explain the features of small amplitude and simple

dynamics usually observed during the electrooxidation of methanol on platinum.

Aiming at comparing the high values observed for the mean CO coverage just discussed with other similar system, we have performed some experiments using formic acid instead of methanol under otherwise identical conditions. Besides the already mentioned richer dynamic behavior, formic acid was chosen because of the considerable amount of spectroscopic data available for this system under oscillatory conditions.⁴⁶⁻⁴⁸ Figure 5 shows potential oscillations obtained under galvanostatic control for the electrooxidation of formic acid on platinum and in sulfuric acid aqueous media. As observed, the potential oscillations are of relaxation-like type and about 5-6 times slower than the ones showed so far for methanol. To the present discussion however, the most important feature is the oscillation amplitude of *ca.* 400 mV. Differently from that observed for methanol, the oscillations during the electrooxidation of formic acid are characterized by the presence of an active state at about 470-480 mV, which is fairly less positive than that of methanol.

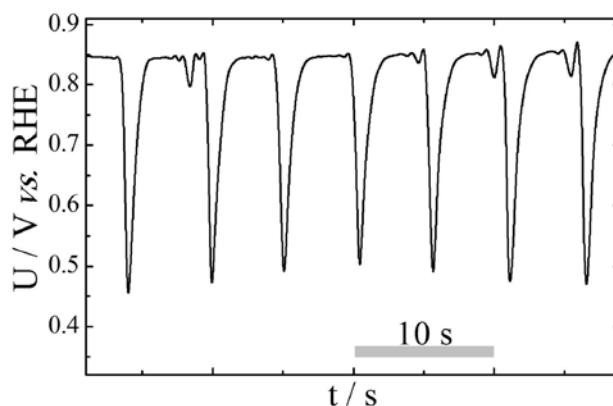


Figure 5. Potential oscillations during the electrooxidation of formic acid on platinum at $I = 4 \text{ mA}$. Electrolyte: $[\text{HCOOH}] = 0.1 \text{ mol L}^{-1}$ and $[\text{H}_2\text{SO}_4] = 0.5 \text{ mol L}^{-1}$.

Similarly to that presented in Figure 4, *in situ* FTIR spectra were also collected along the time series given in Figure 5. A remarkable smaller mean CO coverage (θ_{CO}) of about 0.25-0.30 ML was obtained in this case. Osawa and co-workers^{47,48} studied the potential oscillations in the electrooxidation of formic acid under similar conditions, but using Surface Enhanced Infrared Absorption Spectroscopy (SEIRAS) in a Kretschmann-type attenuated total reflection (ATR) mode, and found similar values for the mean θ_{CO} . Furthermore, Osawa's set up allowed at following the changes in θ_{CO} during the oscillatory electrooxidation of formic acid. For a situation comparable to that given in Figure 5, the authors found variations in the

carbon monoxide coverage from 0.2-0.3 to about 0.35-0.4 monolayers.

It has been proposed that the electrooxidation of small organic molecules proceeds via a so-called dual pathway mechanism⁴⁹⁻⁵⁰⁵¹ in which two parallel reaction pathways occur simultaneously. In this mechanism a *direct pathway* occurs via formation of short living active intermediates which, once formed, are promptly converted to the final product carbon dioxide. In the *indirect pathway*, adsorbed carbon monoxide poisons the electrode surface which is only freed at high overpotentials when CO_{ad} is oxidized by adsorbed oxygenated species, $(\text{H})\text{O}_{\text{ads}}$ species or even activated water $(\text{H}_2)\text{O}_{\text{ads}}$. Mechanistically speaking, oscillations can be explained in terms of the interaction between positive and negative feedback loops acting on the electrode potential. In the autocatalytic loop, the fast adsorption of oxygenated species increases the electrode potential, whereas the negative feedback loop is caused by the slow adsorption of carbon monoxide at lower potentials. As pointed out by Krischer and Varela,²⁶ in spite of the details of the reaction mechanism, the following aspects are known to account for the instabilities in the electrooxidation of small organic molecules: (i) the build up of the adsorbed poison layer (CO_{ad} and possibly other reaction intermediates) along the indirect pathway; (ii) the replenishing of the surface by the reaction between adsorbed poison intermediates (mainly CO_{ad}) and adsorbed oxygenated species; and (iii) the feedback between the total surface coverage on the electrode potential. The difference in the mean θ_{CO} observed during the oscillatory electrooxidation of methanol and formic acid reported here, results of the differences in the rate constants of the reaction steps involved in the oscillatory cycle of each organic molecule.

In contrast to earlier beliefs, Osawa and co-workers^{47,48} suggested formate (adsorbed via both oxygen atoms to two surface sites) as the main active intermediate during formic acid electrooxidation on platinum, and concluded that the rate of formic acid electrooxidation is given in terms of a nonlinear function of the coverages of formate and carbon monoxide. Very importantly, they reported that CO_{ad} acts not only as a poison or site-blocking species but it also inhibits the formate decomposition step. However, using a similar experimental approach, Behm and co-workers⁵² have recently demonstrated that adsorbed bridge-bonded formate species cannot be considered as a reaction intermediate in the main reaction pathway during formic acid electrooxidation on platinum. The authors proposed a triple pathway mechanism including the direct pathway, the indirect pathway, and the formate pathway. In this scenario, adsorbed formate would act as reaction spectator which blocks the catalyst surface in the,

dominant, direct pathway. In the case of methanol, besides carbon monoxide and carbon dioxide, formaldehyde and formic acid are also formed.^{10,14} Moreover, formate has also been observed as an intermediate during methanol electrooxidation on platinum.⁵³ Both the formation and further electrooxidation of those intermediates certainly take part as a current carrier, contributing to the active (non- CO_{ad}) pathway. Under oscillatory conditions, however, this contribution would occur only in the CO free small portion of the surface.

Considering that just a small portion of the surface is in principle involved in the oscillatory cycle during methanol electrooxidation, systematic spectroscopic studies on the influence of different anions in the electrolyte on the oscillatory dynamics would contribute to the elucidation of the mechanism underlying the oscillatory behavior. The thin layer configuration used here has some crucial limitations that could interfere in following, for instance, the precise changes in the oscillations in the CO_{ad} band. In addition, the spectroscopic determination of intermediate species known to be formed during methanol electrooxidation under regular conditions, but in oscillatory regime is a challenging task. Therefore, further studies on the Pt| H_3COH system under oscillatory conditions using ATR-SEIRAS^{47,48} would be of help to uncover the detailed mechanism responsible for the temporal instabilities discussed here.

Conclusions

We have presented results on the oscillatory dynamics found in the electrooxidation of methanol on platinum electrodes in acidic media. The main findings are summarized as follows. Besides potential oscillations, previously unreported current oscillations under potentiostatic control have been found and a bifurcation diagram in the resistance \times voltage plane constructed. Overall, small amplitude oscillations with small modulations in the passive state (high potential or low current state according to the control mode) were observed. Additional information on the mechanistic aspects of the oscillatory dynamics was obtained via *in situ* FTIR spectroscopy experiments using the thin layer configuration. Under galvanostatic control, it was observed that the main surface transformation experienced during the induction period is the increase of the carbon monoxide coverage from about 0.50 (when the system is kept at $U = 50$ mV prior to the current application) to 0.70 ML. The CO_{ad} coverage remains around this value during the potential oscillations and no considerable variations were detected. The mean value of $\theta_{\text{CO}} = 0.70$ is considered very high and implies that only a very small portion of the electrode surface have its population

changing during the oscillation. This could in principle explain the features of small amplitude and poor dynamic behavior usually observed during the electrooxidation of methanol on platinum in acidic media. Further experiments using formic acid instead of methanol and otherwise similar conditions were carried out. As previously reported, the mean CO coverage observed during the oscillation is remarkable lower, and amounts to about 0.25-0.30 ML. This difference in the mean CO coverage was suggested as the main cause for the discrepancies observed in the oscillatory dynamics between the two systems.

Acknowledgments

The authors would like to acknowledge the Fundação de Amparo à Pesquisa do Estado de São Paulo (FAPESP) for financial support (H.V.: 04/04528-0) and for the scholarships (A.L.M.: 05/02409-7, B.C.B.: 07/01575-6, ES: 06/01088-5). B.C.B. also acknowledges CNPq for his previous scholarship. Fruitful discussions with Dr. R. B. de Lima are also strongly acknowledged.

References

1. Carrette, L.; Friedrich, K. A.; Stimming, U.; *Fuel Cells* **2001**, *1*, 5.
2. Arico, A. S.; Srinivasan, S.; Antonucci, V.; *Fuel Cells* **2001**, *1*, 133.
3. Vielstich, W.; *J. Braz. Chem. Soc.* **2003**, *14*, 503.
4. Iwasita, T.; Nart, F. C.; *J. Electroanal. Chem.* **1991**, *317*, 291.
5. Gasteiger, H. A.; Markovic, N.; Ross, P. N.; Cairns, E. J.; *J. Phys. Chem.* **1993**, *97*, 12020.
6. Wilde, C. P.; Zhang, M.; *Electrochim. Acta* **1994**, *39*, 347.
7. Herrero, E.; Chrzanowski, W.; Wieckowski, A.; *J. Phys. Chem.* **1995**, *99*, 10423.
8. Sriramulu, S.; Jarvi, T. D.; Stuve, E. M.; *Electrochim. Acta* **1998**, *44*, 1127.
9. Lu, G. Q.; Chrzanowski, W.; Wieckowski, A.; *J. Phys. Chem. B* **2000**, *104*, 5566.
10. Markovic, N. M.; Ross, P. N.; *Surf. Sc. Rep.* **2002**, *45*, 117.
11. Iwasita, T.; *Electrochim. Acta* **2002**, *47*, 3663.
12. Iwasita, T.; *J. Braz. Chem. Soc.* **2002**, *13*, 401.
13. Iwasita, T. In *Handbook of Fuel Cells – Fundamentals, Technology and Applications*; Vielstich, W.; Gasteiger, H. A.; Lamm, A., eds.; John Wiley & Sons: Chichester, 2003, p. 603.
14. Batista, E. A.; Malpass, G. R. P.; Motheo, A. J.; Iwasita, T.; *J. Electroanal. Chem.* **2004**, *571*, 273.
15. Housmans, T. H. M.; Wonders, A. H.; Koper, M. T. M.; *J. Phys. Chem. B* **2006**, *110*, 10021.
16. Sitta, E.; Varela, H.; *J. Solid State Electrochem.* **2008**, *12*, 559.
17. Buck, R. P.; Griffith, L. R.; *J. Electrochem. Soc.* **1962**, *109*, 1005.
18. Krausa, M.; Vielstich, W.; *J. Electroanal. Chem.* **1995**, *399*, 7.
19. Okamoto, H.; Tanaka, N.; Naito, M.; *J. Phys. Chem. A* **1997**, *101*, 8480.
20. Lee, J.; *PhD Thesis*, Freie Universität Berlin, 2001.
21. Lee, J.; Eickes, C.; Eiswirth, M.; Ertl, G.; *Electrochim. Acta* **2002**, *47*, 2297.
22. Schell, M.; Xu, Y. H.; Amini, A.; *J. Phys. Chem.* **1994**, *98*, 12768.
23. Schell, M.; *J. Electroanal. Chem.* **1998**, *457*, 221.
24. Chen S. L.; Schell, M.; *J. Electroanal. Chem.* **1999**, *478*, 108.
25. Hachkar, M.; Beden, B.; Lamy, C.; *J. Electroanal. Chem.* **1990**, *287*, 81.
26. Krischer, K.; Varela, H. In *Handbook of Fuel Cells – Fundamentals, Technology and Applications*; Vielstich, W.; Gasteiger, H. A.; Lamm, A., eds.; John Wiley & Sons: Chichester, 2003, p. 679.
27. Vielstich, W.; Paganin, V. A.; Lima, F. H. B.; Ticianelli, E. A.; *J. Electrochem. Soc.* **2001**, *148*, A502.
28. Wojtowicz, J.; Marincic, N.; Conway, B. E.; *J. Chem. Phys.* **1968**, *48*, 4333.
29. Schell, M.; Albahadily, F. N.; Safar, J.; Xu, Y.; *J. Phys. Chem.* **1989**, *93*, 4806.
30. Rospel, F.; Nichols, R. J.; Kolb, D. M.; *J. Electroanal. Chem.* **1990**, *286*, 279.
31. Albahadily, F. N.; Schell, M.; *J. Electroanal. Chem.* **1991**, *308*, 151.
32. Okamoto, H.; Tanaka, N.; Naito, M.; *Chem. Phys. Lett.* **1996**, *248*, 289.
33. Markovic, N.; Ross, P. N.; *J. Phys. Chem.* **1993**, *97*, 9771.
34. Strasser, P.; Lubke, M.; Rospel, F.; Eiswirth, M.; Ertl, G.; *J. Chem. Phys.* **1997**, *107*, 979.
35. Tremiliosi-Filho, G.; Jerkiewicz, G.; Conway, B. E.; *Langmuir* **1992**, *8*, 658.
36. Varela, H.; Krischer, K.; *J. Phys. Chem. B* **2002**, *106*, 12258.
37. Iwasita, T.; Nart, F. C.; Vielstich, W.; *C. Ber. Bunsenges. Phys. Chem.* **1990**, *94*, 1030.
38. Strogatz, S.; *Nonlinear Dynamics and Chaos: With Applications to Physics, Biology, Chemistry, and Engineering (Studies in Nonlinearity)*, 1st edition, Perseus Books Group, ISBN 0738204536, 2001.
39. Varela, H.; Krischer, K.; *Catal. Today* **2001**, *70*, 411.
40. Plenge, F.; Varela, H.; Lübke, M.; Krischer, K.; *Z. Phys. Chem.* **2003**, *217*, 365.
41. Sobkowski, J.; Wieckowski, A.; *J. Electroanal. Chem.* **1973**, *41*, 373.
42. Koper, M. T. M.; Sluyters, J. H.; *J. Electroanal. Chem.* **1994**, *371*, 149.

43. Koper, M. T. M. In *Advances in Chemical Physics*; Prigogine, I.; Rice, S. A., eds.; John Wiley & Sons: New York, 1996, p. 161.
44. Krischer, K. In *Modern Aspects of Electrochemistry*; Conway, B. E.; Bockris, J. O. M.; White, R., eds.; Kluwer Academic/Plenum: New York, 1999, p. 1.
45. Strasser, P.; Eiswirth, M.; Koper, M. T. M.; *J. Electroanal. Chem.* **1999**, 478, 50.
46. Honda, Y.; Song, M.-B.; Ito, M.; *Chem. Phys Lett.* **1997**, 273, 141.
47. Samjeske, G.; Osawa, M.; *Ang. Chem. Int. Ed.* **2005**, 44, 5694.
48. Samjeske, G.; Miki, A.; Ye, S.; Yamakata, A.; Mukoyama, Y.; Okamoto, H.; Osawa, M.; *J. Phys Chem. B* **2005**, 109, 23509.
49. Capon, A.; Parsons, R.; *J. Electroanal. Chem.* **1973**, 44, 1.
50. Capon, A.; Parsons, R.; *J. Electroanal. Chem.* **1973**, 44, 239.
51. Capon, A.; Parsons, R.; *J. Electroanal. Chem.* **1973**, 45, 205.
52. Chen, Y. X.; Heinen, M.; Jusys, Z.; Behm, R. J.; *Langmuir* **2006**, 22, 10399.
53. Chen, Y. X.; Miki, A.; Ye, S.; Sakai, H.; Osawa, M.; *J. Am. Chem. Soc.* **2003**, 125, 3680.

Received: October 15, 2007

Web Release Date: April 2, 2008

FAPESP helped in meeting the publication costs of this article.